

A Novel Method for *In Vivo* Visualization of the Microcirculation of the Mandibular Periosteum in Rats

RENÁTA VARGA,* ÁGNES JANOVSKY,*[†] ANDREA SZABÓ,[†] DÉNES GARAB,[†] DÓRA BODNÁR,[†] MIHÁLY BOROS,[†] JÖRG NEUNZEHN,[‡] HANS-PETER WIESMANN,[‡] AND JÓZSEF PIFFKÓ*

*Department of Oral and Maxillofacial Surgery, University of Szeged, Szeged, Hungary; [†]Institute of Surgical Research, University of Szeged, Szeged, Hungary; [‡]Institute of Materials Science, Max Bergmann Center of Biomaterials, TU Dresden, Dresden, Germany

Address for correspondence: Renáta Varga M.D., Ph.D., Department of Oral and Maxillofacial Surgery, University of Szeged, Kálvária sgt. 57, Szeged H-6725, Hungary. E-mail: vargarenata@gmail.com

Received 14 January 2014; accepted 7 March 2014.

ABSTRACT

Objective: The periosteum plays an important role in bone physiology, but observation of its microcirculation is greatly limited by methodological constraints at certain anatomical locations. This study was conducted to develop a microsurgical procedure which provides access to the mandibular periosteum in rats.

Methods: Comparisons of the microcirculatory characteristics with those of the tibial periosteum were performed to confirm the functional integrity of the microvasculature. The mandibular periosteum was reached between the facial muscles and the anterior surface of the superficial masseter muscle at the external surface of the mandibular corpus; the tibial periosteum was prepared by dissecting the covering muscles at the anteromedial surface. Intravital fluorescence microscopy was used to assess the leukocyte–endothelial interactions and the RBCV in the tibial and

mandibular periosteum. Both structures were also visualized through OPS and fluorescence CLSM.

Results: The microcirculatory variables in the mandibular periosteum proved similar to those in the tibia, indicating that no microcirculatory failure resulted from the exposure technique.

Conclusion: This novel surgical approach provides simple access to the mandibular periosteum of the rat, offering an excellent opportunity for investigations of microcirculatory manifestations of dentoalveolar and maxillofacial diseases.

KEY WORDS: mandibular periosteum, intravital microscopy, orthogonal polarization spectral imaging, confocal laser scanning microscopy, rat

Abbreviations used: CLSM, confocal laser scanning microscopy; FITC, fluorescein isothiocyanate; i.v., intravenous; IVM, intravital microscopy; OPS, orthogonal polarization spectral imaging; RBCV, red blood cell velocity.

Please cite this paper as: Varga R, Janovszky Á, Szabó A, Garab D, Bodnár D, Boros M, Neunzehn J, Wiesmann HP, Piffkó J. A novel method for *in vivo* visualization of the microcirculation of the mandibular periosteum in rats. *Microcirculation* 21: 524–531, 2014.

INTRODUCTION

The rich blood supply of the maxillofacial region ensures fast healing of the tissues in the oral cavity. On the other hand, these tissues, and the bones of the jaw in particular, are strikingly prone to local inflammatory complications, ranging from abscess formation to osteomyelitis and osteonecrosis [30]. It is reasonable to assume that functional and morphological impairments of the periosteal microcirculation are critically involved in these processes. This assumption is supported by clinical observations where osteonecrosis and defective angiogenesis of the mucoperiosteal tissues were demonstrated in patients receiving chronic bisphosphonate treatment [37]. In general, the role of the periosteal integrity in bone physiology is well recognized, not

only as it concerns to the maintenance of the vascular supply but also from the aspect of active regulation of the bone metabolism and regeneration. It is similarly well known that successful healing after fractures requires the regeneration of the peri- and endosteal circulations [20]. It follows that periosteal microvascular alterations can be of importance in the pathomechanism of oral diseases associated with a deterioration of tissue perfusion and with inflammatory complications.

The vascular architecture of the intraoral region, including the periosteum, can be examined by imaging methods such as computer tomography, magnetic resonance imaging and to some extent scintigraphy or histology [3,4,11,23]. Nevertheless, these tools are not relevant when dynamic changes or functional aspects of the periosteal microcirculation are to be

investigated. The methods utilized for examinations of the functional characteristics of the microcirculation, such as hemoglobin absorptiometry combined with laser-Doppler flowmetry, may provide information on tissue oxygenation and perfusion, but in this case the tissue mass is rather robust, e.g., the gingiva [21]. If more accurate detection or improved spatial resolution of the microcirculation is needed, fluorescence IVM can provide an opportunity for real-time examination of the microcirculation of superficial layers of different organs. Conventional fluorescence IVM has many advantages. It can visualize not only changes in the efficacy of microvascular perfusion but also leukocyte–endothelial interactions, metabolic variables, or signs of apoptosis [1,17]. For observation of the microcirculation of superficial tissue layers, nonfluorescence techniques such as OPS [14] and sidestream dark-field imaging have also been developed [22]. These methods have the advantage that the use of fluorescence markers is not necessary and this allows a possibility for human applications also in the oral cavity [10,22]. Observation of the periosteal compartment would still necessitate surgical exposure, but the imaging of individual vessels and cells is possible without disturbing their functional characteristics.

The calvarian periosteum can be visualized in experimental settings [32], but examination of the microcirculation of the jaw bones runs into many technical difficulties. We earlier developed methods suitable for visualization of the tibial periosteum and the synovial membrane in the knee joint in rats [15,34], but such approaches were not available for the exposure and *in vivo* investigation of the mandibular periosteum. We therefore considered it important to address this issue, in part to solve the technical problems and in part because the physiology or the pathophysiological reactions of the jaw may differ from those in other bones of the skeleton. Specifically, bisphosphonates have been demonstrated to cause osteonecrosis in the jaw after invasive dental procedures, but such reactions do not occur in the bones of the appendicular skeleton [5,31]. This observation suggests that potentially different microcirculatory reactions may evolve in the periosteum at different anatomical locations. For this reason, we set out to compare the microcirculatory characteristics of the mandibular and the tibial periosteum through the use of a microsurgical approach and microscopic methods that are suitable for *in vivo* visualization of individual microvessels. Firstly, the functional integrity of the mandibular microcirculation was ascertained by using the OPS method, where the use of fluorescent markers is not required (and sampling for biochemical and molecular biological analyses is therefore possible). We used the “gold standard” fluorescence IVM for the determination of perfusion and leukocyte–endothelial interactions. Finally, CLSM was chosen as it offers an opportunity for determination of the *in vivo* histology of tissues (including microvessels)

without sectioning, fixation, and embedding artifacts. The final aim of the study was to provide a comprehensive methodological basis for future investigations targeting the potential microcirculatory manifestations of oral diseases.

MATERIALS AND METHODS

The experiments were performed in full accordance with the NIH Guidelines (Guide for the Care and Use of Laboratory Animals) and approved by the Animal Welfare Committee of the University of Szeged (V/1639/2013).

Animals

Ten male Sprague–Dawley rats were used (the average weight at the time of the experiment was 320 ± 10 g). The animals were anaesthetized intraperitoneally with an initial dose of sodium pentobarbital (45 mg/kg). After cannulation of the trachea, the penile vein was cannulated to administer fluids and drugs (supplementary dose of sodium pentobarbital; 5 mg/kg). During preparation and microcirculatory investigations, the rats were placed in a supine position on a heating pad to maintain the body temperature at 36–37°C.

Surgical Procedures

The fur of the animals in the mandibular region was shaved, and a lateral incision parallel to the incisor tooth was made in the facial skin and the underlying subcutaneous tissue using a careful microsurgical approach under an operating microscope (6× magnification; Carl Zeiss GmbH, Jena, Germany). The masseter muscle consists of superficial and deep parts, the latter being further divided into anterior and posterior sections in rats [9]. The fascia between the anterior part of the deep masseter and the anterior superficial masseter was cut with microscissors (Figure 1A). By this means, the periosteal membrane covering the corpus of the mandible laterally to the incisor tooth was reached and it was gently separated from the covering thin connective tissue (Figure 1B). Stitches with 7.0 monofilament polypropylene microsurgical thread were placed into the surrounding masseter muscles for retraction and better exposure of the region of interest. We applied this surgical approach on both sides of the lower jaw. With this preparation technique, the periosteal microcirculation of the mandible could be examined by *in vivo* microscopic methods at the anterior margin of the molar region.

For comparison of the characteristics of the mandibular microcirculation with those of the tibial periosteum, the medial/anterior surface of the tibia was exposed by complete transection of the anterior gracilis muscle with microscissors, and careful atraumatic microsurgical removal of the connective tissue covering the tibial periosteum (Figure 1C,D) [34]. These dissections were performed on both sides to permit parallel observations of intravascular and topically applied fluorescence tracers (see later).

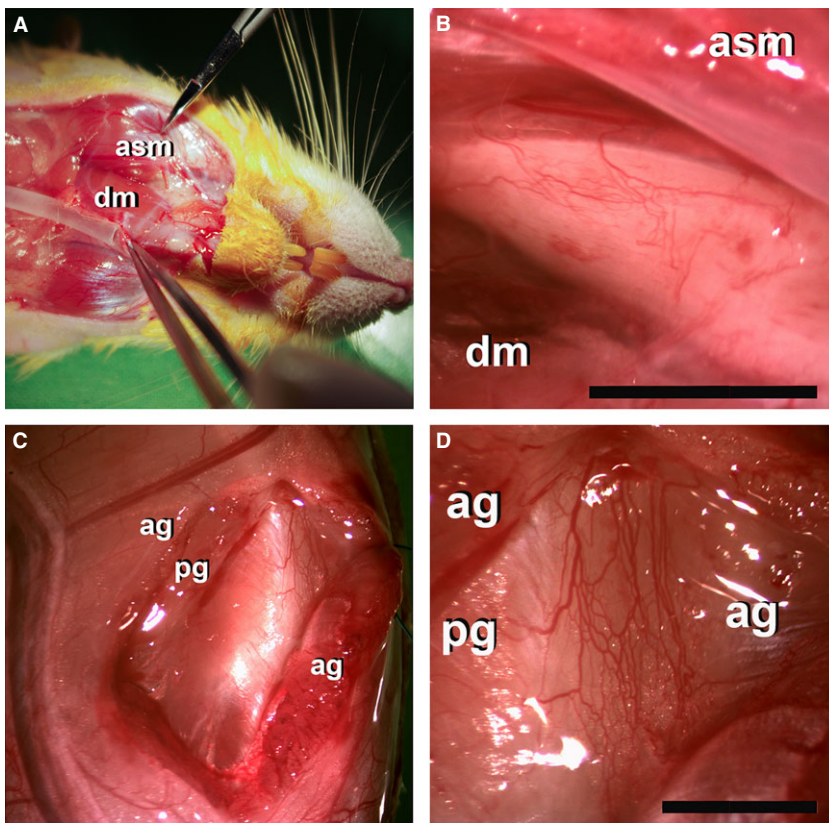


Figure 1. Exposure of the mandibular and tibial periosteum for *in vivo* microscopic examinations. Access to the mandibular periosteum was achieved by making a lateral incision parallel to the incisor tooth in the facial skin and the underlying subcutaneous tissue, which was followed by gentle separation of the fascia between the anterior part of the deep masseter (dm) and the anterior superficial masseter (asm) muscles (**A, B**). Finally, the thin connective tissue covering the periosteum was gently incised with microscissors. By this means, the periosteal membrane covering the corpus of the mandible laterally to the incisor tooth was reached. The tibial periosteum was reached by transecting the anterior gracilis (ag) muscle completely in the middle (and a part of the posterior gracilis muscle [pg] too) and gently removing the thin connective tissue covering the periosteum (**C, D**). The bar denotes 2500 μm .

Experimental Protocol

After surgical exposure of the mandibular and tibial periosteum on both sides, recordings were performed on the right side with OPS, which does not require any fluorescence labeling (see later) (Figure 2A,B). After this, the animals received *i.v.* injections of FITC-labeled erythrocytes (0.2 mL; Sigma Aldrich, St. Louis, MO, USA) (Figure 3A,B) [27] and rhodamine-6G (0.2%, 0.1 mL; Sigma Aldrich) for the staining of leukocytes (Figure 3C,D), and IVM recording was performed at the previous locations. Subsequently, 50 μL of the nuclear dye acriflavin (1 mM) was applied topically to the tibial periosteal surface on the left side and was rinsed off with warm physiological saline solution after an exposure time of one minute, and then CLSM recording

was performed (Figure 4B). The same staining procedure was carried out for the mandible on the left side (Figure 4A). This was followed by an *i.v.* injection of the plasma dye FITC-dextran 150 kDa (*i.v.* 0.3 mL, 20 mg/mL solution dissolved in saline; Sigma Aldrich), and CLSM (Figure 4C,D) and IVM recordings (Figure 3E,F) were made on the tibia and the mandible on the right side five minutes after injection of the tracer.

OPS Technique

The exposed periosteum of the corpus of the mandible or the tibial periosteum on the right side was horizontally positioned on an adjustable stage and superfused with 37°C saline. The periosteal membranes were first visualized with

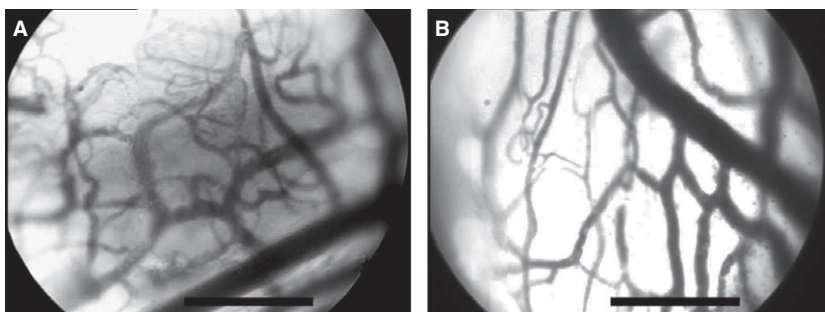


Figure 2. Micrographs showing the mandibular (**A**) and tibial periosteum (**B**) made with the OPS technique. The bar denotes 200 μm .

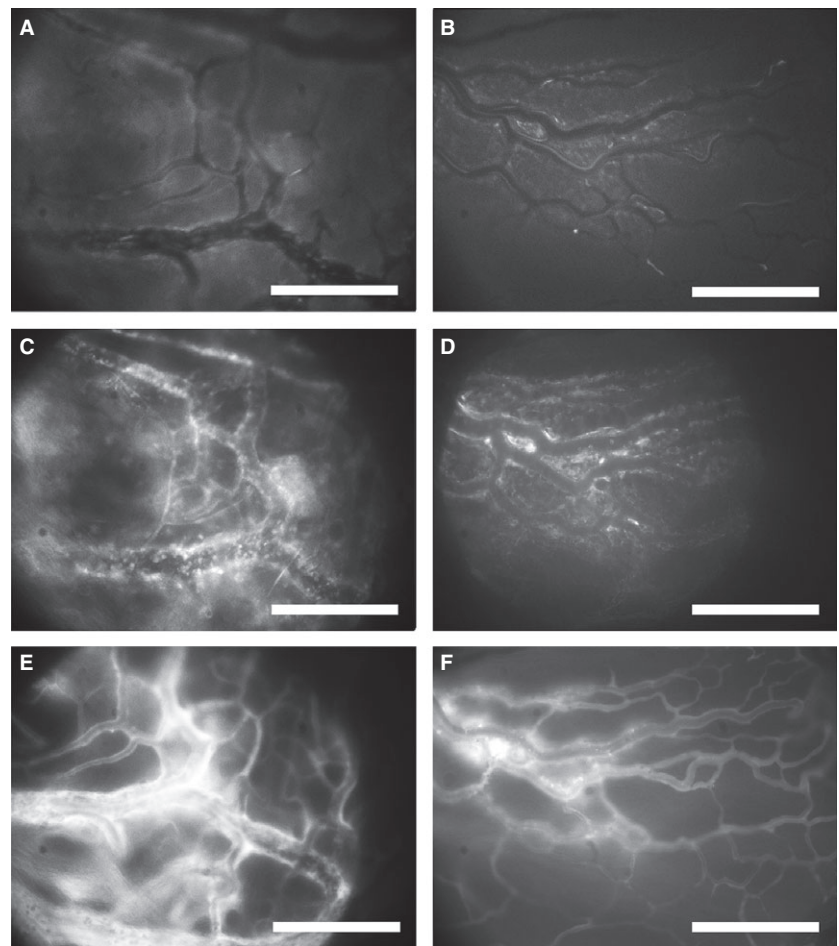


Figure 3. Fluorescence intravital microscopic images of the mandibular (**A, C, E**) and the tibial periosteum (**B, D, F**), involving FITC-labeled erythrocytes (**A, B**), rhodamine 6G-labeled neutrophil leukocytes (**C, D**), and FITC-dextran-labeled plasma (**E, F**). The bar denotes 200 μm .

an OPS device (CytoscanTM; Cytometrics, Philadelphia, PA, USA), which provides optimal imaging of the microvascular structures at a chosen focus level [penetration depth: approx. 200 μm ; 11] (Figure 2A,B). This technique utilizes epi-illumination with linearly polarized light at 548 nm (which is the isobestic point of oxy- and deoxyhemoglobin) to visualize hemoglobin-containing structures without the additional use of a fluorochrome. Images were recorded on a SVHS video recorder (Panasonic AG-MD 830; Matsushita Electric Industrial Co., Tokyo, Japan) and a personal computer.

Fluorescence IVM

The periosteal microcirculation was visualized by IVM (penetration depth: approx. 250 μm ; Zeiss Axiotech Vario 100HD microscope; 100-W HBO mercury lamp; Acroplan 20 \times /0.5 N.A. W; Carl Zeiss GmbH, Jena, Germany). Images from three–four fields of the mandibular and the tibial periosteum (Figure 3) were recorded with a charge-coupled device video camera (Teli CS8320Bi; Toshiba Teli Corporation, Osaka, Japan) attached to an S-VHS video recorder

(Panasonic AG-MD 830; Matsushita Electric Industrial Co.) and a personal computer (see labeling techniques above).

Fluorescence CLSM

Confocal imaging of the surface of the mandibular and tibial periosteum was performed with a Five1 Optiscan device (Optiscan Pty. Ltd., Melbourne, Vic., Australia) (Figure 4). *In vivo* histology was employed by placing the Optiscan probe on the surface of the periosteal membranes and by changing the focus level through virtual sections of 7 μm during the confocal imaging (penetration depth: 0–250 μm). Cell nuclei were first stained with topically applied acriflavin (see above) on the left side, and this was followed by recordings on the contralateral side after i.v. injection of the intravascular tracer FITC-dextran (see above). Images were stored on a personal computer provided by the manufacturer.

Video Analysis

Quantitative evaluation of the microcirculatory parameters was performed off-line by the frame-to-frame analysis of the

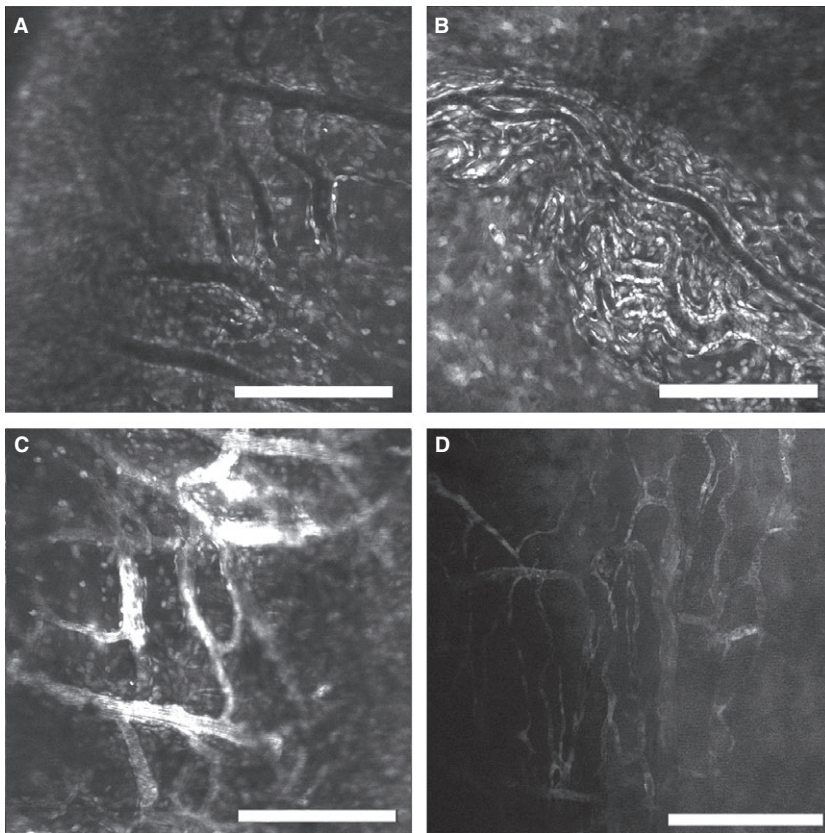


Figure 4. Confocal laser scanning microscopic images of the mandibular (**A, C**) and tibial periosteum (**B, D**). Cell nuclei were labeled by the topical application of acriflavin (left side) (**A, B**). Images were also taken at both structures on the right sides after the i.v. injection of FITC-dextran (**C, D**). The bar denotes 200 μm .

videotaped images taken for IVM and OPS (IVM Software; Pictron Ltd, Budapest, Hungary). Leukocyte–endothelial cell interactions were analyzed at least in four postcapillary venules per rat. Rolling leukocytes were defined as cells moving with a velocity less than 40% of that of the erythrocytes in the centerline of the microvessel and passing through the observed vessel segment within 30 seconds, and are given as the number of cells per second per vessel circumference. Adherent leukocytes were defined as cells that did not move or detach from the endothelial lining within an observation period of 30 seconds and are given as the number of cells per mm^2 of endothelial surface, calculated from the diameter and length of the vessel segment. RBCV ($\mu\text{m}/\text{s}$) was determined by frame-to-frame analysis of 5–6 consecutive video-captured images taken after labeling of the erythrocytes (see above).

Statistical Analysis

The statistical analysis was performed with a statistical software package (SigmaStat for Windows, Jandel Scientific, Erkrath, Germany). Within the IVM data, RBCV values in the capillaries and the extents of rolling and adherence of leukocytes in the postcapillary venules of the mandibular and tibial periosteum were compared by using the Student's *t*-test. Comparisons within the RBCV values measured with

IVM and OPS were also made with the Student's *t*-test. *p* values <0.05 were considered significant.

RESULTS

With the reported preparation technique, the anterior surface of the tibial periosteum provides a larger observation field (ranging between 8.89 and 9.88 mm^2) (Figure 1D) than that of the exposed mandibular region (ranging between 8.03 and 9.18 mm^2) (Figure 1B). Furthermore, the entire exposed tibial periosteal surface can be examined by different *in vivo* microscopic methods, whereas only approximately one third of the mandibular periosteum (i.e., its anterior part) can easily be reached by the relatively robust objectives. The vascular density reached $0.0182 \pm 0.0011/\mu\text{m}$ in case of the tibia and was $0.0193 \pm 0.0008/\mu\text{m}$ in the mandibular periosteum. The arterioles, capillaries, and venules can be distinguished on the basis of vessel diameters and the direction of flow of moving elements (plasma or red blood cells) within them. Within the mandibular periosteum, the vascular network consisted mainly of arterioles and venules, but a few capillaries and mostly venules were present in the tibial periosteum (as depicted in Figures 2–4).

IVM demonstrated that the RBCV values were similar in the two capillary beds ($827.5 \pm 30.1 \mu\text{m}/\text{s}$ in the mandibular

and $739.0 \pm 37.7 \mu\text{m/s}$ in the tibial periosteum) (Table 1). The OPS technique revealed similar RBCV values (data not shown). The IVM data did not indicate any significant differences in the magnitude of the leukocyte–endothelial cell interactions between the two locations (Table 1).

The CLSM method was applied to stain the cell nuclei of the vascular compartment (Figure 4A,B). The vascular organization was also visualized when intravascular dye (FITC-dextran) was employed (Figure 4C,D).

At the end of the experiments, tissue specimens were harvested for histology. The tibial periosteum appeared to be more strongly attached to the underlying bone than that in the mandible.

DISCUSSION

Studies of the microcirculation in the oral region gained considerable attention when the predictive value of mucosal perfusion deficits was demonstrated in septic shock patients [33,35]. Another intraoral manifestation of a systemic menace was revealed during cardiac surgery [2] and the intraoral microcirculation was demonstrated to correlate well with the gastrointestinal perfusion changes [35]. The periosteal microcirculatory aspects of systemic and intraoral diseases, however, have been far less well clarified. These above human observations became possible by the development of methods which provide quantitative information on individual vessels without the need for the use of fluorescent tracers (i.e., OPS or sidestream dark-field methods). High spatial resolution is an advantage of intravital microscopic methods in general, but the relatively low penetration depth restricts the examination to the superficial layers such as the mucosal or gingival/mucosal surfaces in the oral cavity.

As a major source of osteoprogenitor cells, the periosteum of the jaw bones has a high impact in the pathogenesis of various orofacial diseases, but specific, real-time examination of its microcirculation can be performed only after surgical exposure of this structure. As a result, the periosteal microcirculation has been examined in only a relatively limited number of studies of the tibia [26,28,34,38] or the

calvaria [32], and we are aware of only one study in the maxilla–mandibular region, in rabbits [25]. All these latter studies involved the use of conventional fluorescence IVM which (as opposed to OPS) also makes possible the investigation of microcirculatory perfusion, permeability, and leukocyte–endothelial interactions. In this study, we developed a surgical approach to the mandibular periosteum. When a rodent model is to be established, similarities to the human anatomy should first be ascertained. The most accessible region, where the periosteum is situated most superficially, is the area medial to the parotideomasseteric region [9]. This region, between the superficial masseter muscles and the mentum, just laterally to the ever-growing incisor tooth of the rat, can be approached by incising the skin and subcutaneous tissue. We gained access to the periosteum next to the anterior part of the superficial masseter muscle in the area where this muscle adheres to the ventral margin of the mandible. It was considered important to proceed laterally to the continuously growing incisor teeth so as to avoid any potential functional dissimilarities to the human characteristics.

The fluorescence IVM data revealed that the mandibular microcirculatory variables are similar to those seen in the tibia. It should be added that the preparation was stable for approximately four hours in preliminary experiments, when only IVM was employed (data not shown). In the case of CLSM, the potential toxic effects of topically applied nuclear dyes would probably influence the microcirculation in the long run, and examination may be therefore preferably be restricted to one time point only. As regards the periosteal microcirculation, examination of the effects of surgical trauma of the tibia [38] and the maxilla [25] is a possible target for IVM methods. Such questions can also be answered by using the present exposure technique. Moreover, the consequences of tooth extraction (particularly of first molars) and the subsequent osteogenesis on the periosteal microcirculatory reactions may also be examined. In previous studies, osteogenesis-related capillary density changes (by OPS) [19] and leukocyte–endothelial interactions in experimental periodontitis (by IVM) [7] were examined in the

Table 1. Microcirculatory parameters: RBCV in the capillaries, and leukocyte rolling, and sticking in the postcapillary venules of the mandibular and tibial periosteum in rats as determined by the OPS technique and fluorescence IVM

Method Parameter	OPS RBCV ($\mu\text{m/s}$)	IVM		
		RBCV ($\mu\text{m/s}$)	Rolling (/mm/s)	Sticking (/mm ²)
Mandible	736.6 ± 26.7	827.5 ± 30.1	46.6 ± 5.8	13.4 ± 4.4
Tibia	723.7 ± 39.2	739.0 ± 37.7	56.9 ± 11.5	18.5 ± 3.9

Mean values \pm SEM are presented.

mucosa, but never in the periosteum. Furthermore, the present model appears suitable for CLSM; the penetration of intranuclear dyes for the examination of angiogenesis and apoptosis is also possible. CLSM has previously been employed in the oral mucosa to visualize intraoral mucosal lesions, tumors [12], borders of malignancies, and resection margins [6,16,29].

The jaws are particularly prone to inflammatory complications (e.g., periodontitis or abscess), as they can be sensitively exposed to the external environment in the immediate vicinity of the teeth. The IVM approach can be a particularly valuable tool for the examination of oral inflammatory processes. In consequence of the relatively high penetration depth of laser light, laser-Doppler flowmetry has been used for the detection of mucosal/gingival inflammatory processes. As examples, the consequences of periodontal access flap surgery and inflammation have been detected in the gingiva [18,24] and in the pulpar blood flow [36]. With use of the proposed method, such inflammatory complications could also be examined using the mandibular periosteum.

This study demonstrated certain differences in architecture in the mandibular and the tibial periosteum. Specifically, the venules are proved to be the predominant structures in the examined anteromedial surface of the tibia, whereas arterioles were also detected in the mandible. Differences within the skeletal system were reported by Chanavaz, who found that the jaw microcirculation has a higher number of anastomoses and a greater impact on the centromedullary circulation as opposed to the long bones of the skeleton [8]. A corrosion cast study similarly revealed lower numbers of capillaries and arterioles in the periosteal compartment than in the gingival compartment, which is characterized by a rich capillary network [23]. At the present stage, the impact of our observations cannot be fully assessed and the potential regional differences should also be taken into account: We earlier demonstrated [13] that the anterolateral side of the tibia (which was used for a myocutaneous flap model by Rücker *et al.* [26]) has more capillaries than on the anteromedial side. We consider that the higher density of venules may predispose to microcir-

culatory inflammatory complications, e.g., the transmigration of neutrophil leukocytes through the postcapillary venules.

In summary, the new microsurgical approach presented provides access to the periosteal microcirculation in the rat mandible. We compared the mandibular microcirculatory variables with those of a standard and stable tibial model by using fluorescence IVM to ascertain that this new technique does not cause microcirculatory disturbances or inflammatory complications. It was demonstrated that this exposure procedure makes the mandibular periosteum accessible for OPS and CLSM examinations. It is anticipated that this model and the investigation of mandibular microcirculatory alterations may contribute to a better understanding of maxillofacial or dentoalveolar diseases.

PERSPECTIVE

The maxillofacial region is particularly prone to inflammatory reactions. The present rat model using IVM techniques should be useful in further studies exploring the periosteal microcirculation, pathophysiological mechanisms of bone regeneration, dentoalveolar diseases, and drug-related complications such as mandibular osteonecrosis.

ACKNOWLEDGMENTS

This publication/presentation is supported by the European Union and cofunded by the European Social Fund. Project title: "Telemedicine-focused research activities in the field of Mathematics, Informatics and Medical Sciences". Project number: TÁMOP-4.2.2.A-11/1/KONV-2012-0073. Further supporting research grants are as follows: TÁMOP 4.2.4.A/2-11-1-2012-0001, TÁMOP-4.2.2.A-11/1/KONV-2012-0035 and OTKA – 109388.

CONFLICT OF INTEREST

The authors declare that they have no conflict of interest.

REFERENCES

1. Abshagen K, Eipel C, Menger MD, Vollmar B. Comprehensive analysis of the regenerating mouse liver: an in vivo fluorescence microscopic and immunohistological study. *J Surg Res* 134: 354–362, 2006.
2. Bauer A, Kofler S, Thiel M, Eifert S, Christ F. Monitoring of the sublingual microcirculation in cardiac surgery using orthogonal polarization spectral imaging: preliminary results. *Anesthesiology* 107: 939–945, 2007.
3. Berggren A, Weiland AJ, Ostrup LT, Dorfman H. Microvascular free bone transfer with revascularization of the medullary and periosteal circulation or the periosteal circulation alone. A comparative experimental study. *J Bone Joint Surg Am* 64: 73–87, 1982.
4. Bhatt R, Lauder I, Finlay DB, Allen MJ, Belton IP. Correlation of bone scintigraphy and histological findings in medial tibial syndrome. *Br J Sports Med* 34: 49–53, 2000.
5. Blazsek J, Dobó Nagy C, Blazsek I, Varga R, Vecsei B, Fejérdy P, Varga G. Aminobisphosphonate stimulates bone regeneration and enforces consolidation of titanium implant into a new rat caudal vertebrae model. *Pathol Oncol Res* 15: 567–577, 2009.
6. Capodiferro S, Maiorano E, Lojudice AM, Scarpelli F, Favia G. Oral laser surgical pathology: a preliminary study on the clinical advantages of diode laser and on the histopathological features of specimens evaluated by conventional and confocal laser scanning microscopy. *Minerva Stomatol* 57: 1–6, 6–7, 2008.

7. Carvalho RR, Pellizzon CH, Justulin L, Jr, Felisbino SL, Vilegas W, Bruni F, Lopes-Ferreira M, Hiruma-Lima CA. Effect of mangiferin on the development of periodontal disease: involvement of lipoxin A4, anti-chemotaxic action in leukocyte rolling. *Chem Biol Interact* 179: 344–350, 2009.
8. Chanavaz M. Anatomy and histophysiology of the periosteum: quantification of the periosteal blood supply to the adjacent bone with 85Sr and gamma spectrometry. *J Oral Implantol* 21: 214–219, 1995.
9. Cox PG, Jeffery N. Reviewing the morphology of the jaw-closing musculature in squirrels, rats, and guinea pigs with contrast-enhanced microCT. *Anat Rec (Hoboken)* 294: 915–928, 2011.
10. De Backer D, Donadello K, Sakr Y, Ospina-Tascon G, Salgado D, Scolletta S, Vincent JL. Microcirculatory alterations in patients with severe sepsis: impact of time of assessment and relationship with outcome. *Crit Care Med* 41: 791–799, 2013.
11. Fayad LM, Kamel IR, Kawamoto S, Bluemke DA, Frassica FJ, Fishman EK. Distinguishing stress fractures from pathologic fractures: a multimodality approach. *Skeletal Radiol* 34: 245–259, 2005.
12. Franz M, Hansen T, Borsi L, Geier C, Hyckel P, Schleier P, Richter P, Altendorf-Hofmann A, Kosmehl H, Berndt A. A quantitative colocalization analysis of large unspliced tenascin-C(L) and laminin-5/gamma2-chain in basement membranes of oral squamous cell carcinoma by confocal laser scanning microscopy. *J Oral Pathol Med* 36: 6–11, 2007.
13. Greksa F, Tóth K, Boros M, Szabó A. Periosteal microvascular reorganization after tibial reaming and intramedullary nailing in rats. *J Orthop Sci* 17: 477–483, 2012.
14. Groner W, Winkelmann JW, Harris AG, Ince C, Bouma GJ, Messmer K, Nadeau RG. Orthogonal polarization spectral imaging: a new method for study of the microcirculation. *Nat Med* 5: 1209–1212, 1999.
15. Hartmann P, Erős G, Varga R, Kaszaki J, Garab D, Németh I, Rázga Z, Boros M, Szabó A. Limb ischemia-reperfusion differentially affects the periosteal and synovial microcirculation. *J Surg Res* 178: 216–222, 2012.
16. Haxel BR, Goetz M, Kiesslich R, Gosepath J. Confocal endomicroscopy: a novel application for imaging of oral and oropharyngeal mucosa in human. *Eur Arch Otorhinolaryngol* 267: 443–448, 2010.
17. Horie Y, Wolf R, Miyasaka M, Anderson DC, Granger DN. Leukocyte adhesion and hepatic microvascular responses to intestinal ischemia/reperfusion in rats. *Gastroenterology* 111: 666–673, 1996.
18. Kerdvongbudit V, Vongsavan N, So-Ampon S, Hasegawa A. Microcirculation and micromorphology of healthy and inflamed gingivae. *Odontology* 91: 19–25, 2003.
19. Lindeboom JA, Mathura KR, Milstein DM, Ince C. Microvascular soft tissue changes in alveolar distraction osteogenesis. *Oral Surg Oral Med Oral Pathol Oral Radiol Endod* 106: 350–355, 2008.
20. Macnab I, Dehoas WG. The role of periosteal blood supply in the healing of fractures of the tibia. *Clin Orthop* 105: 27–33, 1974.
21. Milstein DM, Cheung YW, Žiūkaitė L, Ince C, van den Akker HP, Lindeboom JA. An integrative approach for comparing microcirculation between normal and alveolar cleft gingiva in children scheduled for secondary bone grafting procedures. *Oral Surg Oral Med Oral Pathol Oral Radiol* 115: 304–309, 2013.
22. Milstein DM, Lindeboom JA, Ince C. Intravital sidestream dark-field (SDF) imaging is used in a rabbit model for continuous noninvasive monitoring and quantification of mucosal capillary regeneration during wound healing in the oral cavity: a pilot study. *Arch Oral Biol* 55: 343–349, 2010.
23. Nobuto T, Yanagihara K, Teranishi Y, Minamibayashi S, Imai H, Yamaoka A. Periosteal microvasculature in the dog alveolar process. *J Periodontol* 60: 709–715, 1989.
24. Retzepi M, Tonetti M, Donos N. Gingival blood flow changes following periodontal access flap surgery using laser Doppler flowmetry. *J Clin Periodontol* 34: 437–443, 2007.
25. Rucker M, Binger T, Deltcheva K, Menger MD. Reduction of midfacial periosteal perfusion failure by subperiosteal versus suprapariosteal dissection. *J Oral Maxillofac Surg* 63: 87–92, 2005.
26. Rucker M, Roesken F, Vollmar B, Menger MD. A novel approach for comparative study of periosteum, muscle, subcutis, and skin microcirculation by intravital fluorescence microscopy. *Microvasc Res* 56: 30–42, 1998.
27. Ruh J, Ryschich E, Secchi A, Gebhard MM, Glaser F, Klar E, Herfarth C. Measurement of blood flow in the main arteriole of the villi in rat small intestine with FITC-labeled erythrocytes. *Microvasc Res* 56: 62–69, 1998.
28. Schaser KD, Zhang L, Haas NP, Mittlmeier T, Duda G, Bail HJ. Temporal profile of microvascular disturbances in rat tibial periosteum following closed soft tissue trauma. *Langenbecks Arch Surg* 388: 323–330, 2003.
29. Scivetti M, Lucchese A, Ficarra G, Giuliani M, Lajolo C, Maiorano E, Favia G. Oral pulse granuloma: histological findings by confocal laser scanning microscopy. *Ultrastruct Pathol* 33: 155–159, 2009.
30. Scoletta M, Arduino PG, Dalmasso P, Broccoletti R, Mozzati M. Treatment outcomes in patients with bisphosphonate-related osteonecrosis of the jaws: a prospective study. *Oral Surg Oral Med Oral Pathol Oral Radiol Endod* 110: 46–53, 2010.
31. Stadelmann VA, Gauthier O, Terrier A, Bouler JM, Pioletti DP. Implants delivering bisphosphonate locally increase periprosthetic bone density in an osteoporotic sheep model. A pilot study. *Eur Cell Mater* 16: 10–16, 2008.
32. Stuehmer C, Schumann P, Bormann KH, Laschke MW, Menger MD, Gellrich NC, Rucker M. A new model for chronic in vivo analysis of the periosteal microcirculation. *Microvasc Res* 77: 104–108, 2009.
33. Top AP, Ince C, de Meij N, van Dijk M, Tibboel D. Persistent low microcirculatory vessel density in nonsurvivors of sepsis in pediatric intensive care. *Crit Care Med* 39: 8–13, 2011.
34. Varga R, Török L, Szabó A, Kovács F, Keresztes M, Varga G, Kaszaki J, Boros M. Effects of colloid solutions on ischemia-reperfusion-induced periosteal microcirculatory and inflammatory reactions: comparison of dextran, gelatin, and hydroxyethyl starch. *Crit Care Med* 36: 2828–2837, 2008.
35. Verdant CL, De Backer D, Bruhn A, Clausi CM, Su F, Wang Z, Rodriguez H, Pries AR, Vincent JL. Evaluation of sublingual and gut mucosal microcirculation in sepsis: a quantitative analysis. *Crit Care Med* 37: 2875–2881, 2009.
36. Verdickt GM, Abbott PV. Blood flow changes in human dental pulps when capsaicin is applied to the adjacent gingival mucosa. *Oral Surg Oral Med Oral Pathol Oral Radiol Endod* 92: 561–565, 2001.
37. Wehrhan F, Stockmann P, Nkenke E, Schlegel KA, Guentsch A, Wehrhan T, Neukam FW, Amann K. Differential impairment of vascularization and angiogenesis in bisphosphonate-associated osteonecrosis of the jaw-related mucoperiosteal tissue. *Oral Surg Oral Med Oral Pathol Oral Radiol Endod* 112: 216–221, 2011.
38. Zhang L, Bail H, Mittlmeier T, Haas NP, Schaser KD. Immediate microcirculatory derangements in skeletal muscle and periosteum after closed tibial fracture. *J Trauma* 54: 979–985, 2003.